Article

EEG Waveform Analysis of P300 ERP with applications to Brain Computer Interfaces

Rodrigo Ramele [1,†], Ana Julia Villar [1] and Juan Miguel Santos [1*]

[1] Computer Engineering Department, Instituto Tecnológico de Buenos Aires (ITBA); info@itba.edu.ar

* Correspondence: rramele@itba.edu.ar; Tel.: +54-9-11-4193-9382

† Current address: C1437FBH Lavarden 315, Ciudad Autónoma de Buenos Aires, Argentina

1   **Abstract:** The Electroencephalography (EEG) is not just a mere clinical tool anymore. It has become
2   the de-facto mobile, portable, non-invasive brain imaging sensor to harness brain information in real
3   time and translating or decoding brain signals that can be used to diagnose disease or implement
4   Human Computer Interaction devices. The automatic processing approach which is based on using
5   quantitative algorithms to detect the cloaked information buried in the signal, outshines the research
6   done by the clinical EEG community which was based intensively on EEG waveforms and the
7   structure of signal plots. Hence, the purpose of this work is to establish a bridge to fill this gap
8   by doing a review and description of the procedures that have been used to detect patterns in the
9   electroencephalographic waveforms, and to perform a benchmarking analysis of them.

10 **Keywords:** electroencephalography (EEG); ERP,BCI,waveform, signal structure

---

0. Introduction

12   Current society is demanding technology to provide the means to realize the utopia of social
13 inclusion for people with disabilities [1]. Additionally, as societies are aging [2] the incidence of
14 neuromuscular atrophies, strokes and other invalidating diseases is increasing. Concurrently, the
15 digital revolution and the pervasiveness of digital gadgets have modified the way people interact
16 with the environment through these devices [3]. All this human computer interaction is based on
17 muscular movement [4], but these trends are pushing this boundary beyond the confines of the body
18 and beyond the limitation of human motion. A new form of human machine communication which
19 directly connects the Central Nervous System (CNS) to a machine or computer device is currently
20 being developed: Brain Machine Interfaces (BMI), Brain Computer Interfaces (BCI) or Brain-Neural
21 Computer Interfaces (BNCI).

22   At the center of all this hype, we can find a hundredth year old technology, rock-solid as a
23 diagnosis tool, which greatly benefited from the shrinkage of sensors, the increase in computer
24 power and the widespread development of wireless protocols and advanced electronics: the
25 Electroencephalogram (EEG) [5].

26   EEG sensors are wearable [6] non-invasive, portable and mobile [7], with excellent temporal
27 resolution, and acceptable spatial resolution [8]. This humble diagnosis device is been transformed
28 into currently the best approach to detect, out-of-the lab in an ambulatory context, information from
29 the Central Nervous System and to use that information to volitionally drive cars, steer drones, write
30 emails, or control wheelchairs [9].

31   The clinical and historical tactic to analyze EEG signals were based on detecting visual patterns
32 out of the EEG trace or polygraph[8]: multichannel signals were extracted and continuously plotted
33 over a piece of paper. Electroencephalographers or Electroencephalography technician have decoded

and detected patterns along the signals by visually inspecting them [5]. Nowadays clinical EEG still remains a visually interpreted test [8].

In contrast, automatic processing, or quantitative EEG (qEEG), was based first on analog electronic devices [10] and later on computerized digital processing methods [11]. They implemented algorithmically complex procedures to decode the information associated with a clinical condition, or even some higher cognitive state [9]. The best materialization of the automatic processing of EEG signals rests in the BCI discipline, where around 71.2% is based on noninvasive EEG [4].

Hence, the traditional and knowledgeable approach was mainly overshadow particularly in BCI Research, and the waveform of the EEG was replaced by pragmatic procedures that were difficult to link to existing clinical EEG knowledge. We aim to help fix this gap by providing a review of the methods which emphasize the waveform, the shape of the EEG signal and that can help to decode them in a supervised and semi-automated way.

The aim of this study is twofold: first to review current literature of EEG processing techniques which are based on analysis of the waveform. The second is to evaluate and study these methods by analyzing its classification performance against a pseudo-real dataset. We believe that the importance of waveform analysis methods, as described here, is that by using this methodology, collaboration could be fostered because there is a clear description and characterization of the signal, where the extensive literature which explores clinical EEG can be reviewed from the same shared perspective [12,13].

This article unfolds as follows: Section 1 will provide a brief introduction to EEG and the particularities of the EEG waveform characterization. Section 2.1 will explain the algorithms based on the waveform that will be analyzed. In Section 2.6 the experimentation procedure will be explained. Results will be presented in Section 3 and finally Discussion and Conclusions will be established in the final sections.

1. Electroencephalography

The Electroencephalography consists on the measurement of small variations of electrical currents over the scalp. It is one of the most widespread used methods to capture brain signals and was initially developed by Hans Berger in 1924 and has been extensively used for decades to diagnose neural diseases and other medical conditions.

The first characterization that Dr. Berger detected was the Visual Cortical Alpha Wave, the *Berger Rythm* [11]. He understood that the amplitude and shape of this rhythm was coherently associated to a cognitive action (eyes closing). We should ask ourselves if the research advancement that came after that discovery would have happened if it weren't so evident that the shape alteration was due to a very simple and verifiable cognitive process.

The EEG signal is a highly complex multi-channel time-series. It can be modeled as a linear stochastic process with great similarities to noise [14]. It is measured in microvolts, and those slightly variations are contaminated with heavy endogenous artifacts and exogenous spurious signals. Figure 1 show 5 seconds of a sample 8-channel EEG signal.
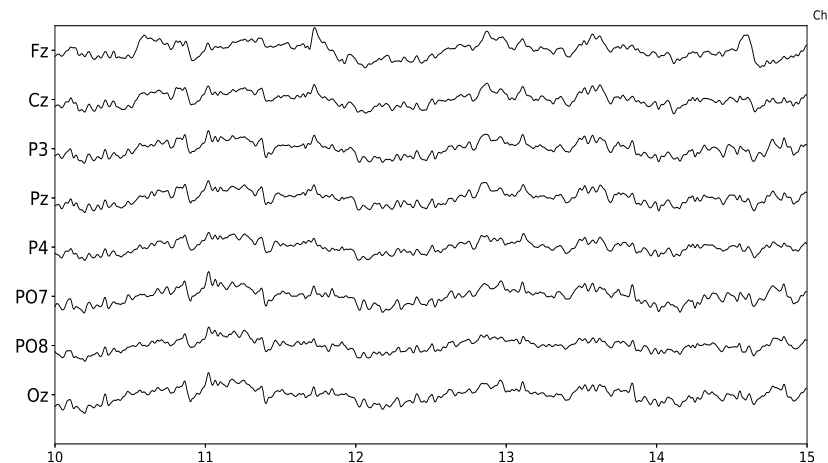
Figure 1. Sample EEG signal obtained from g.Tec g.Nautilus. Time axis is in seconds and five seconds are displayed. The eight channels provided by this device are shown.

The device that captures these small variations in potential differences over the scalp is called the Electroencephalograph. Electrodes are located in predetermined positions over the head, usually embedded in saline solutions to facilitate the electrophysiological interface and are connected to a differential amplifier with a high gain which allows the measurement of tiny signals. Although initially analog devices were developed and used, nowadays digital versions connected directly to a computer are pervasive. A detailed explanation on the particularities and modeling of EEG can be obtained from [15], and a description of its electrophysiological aspects from [16].

Overall, EEG signals can be described by their phase, amplitude, frequency and *waveform*. The following elements regularly characterize EEG signals:

- Artifacts: These are signal sources which are not generated from the CNS, but can be detected from the EEG signal. They are called endogenous or physiological when they are generated from a biological source like face muscles, ocular movements, etc., and exogenous or non-physiological when they have an external electromagnetic source like line induced currents or electromagnetic noise[17].
- Non-Stationarity: the statistical parameters that describe the EEG as a random process are not conserved through time, i.e. its mean and variance, and any other higher-order moments are not time-invariant [11].
- DC drift and trending: in EEG jargon, which is derived from concepts of electrical amplifiers theory, Direct Current (DC) refers to very low frequency components of the EEG signal which varies around a common center, usually the zero value. DC drift means that this center value drifts in time. Although sometimes considered as a nuisance that needs to get rid of, it is known that very important cognitive phenomena like Slow Cortical Potentials or Slow Activity Transients in infants do affect the drift and can be used to understand some particular brain functioning [5].
- Basal EEG activity: the EEG is the compound summation of myriads of electrical sources from the CNS. These sources generate a baseline EEG which shows continuous activity with a small or null relation with any concurrent cognitive activity or task.
- Inter-subject and intra-subject variability: EEG can be affected by the person's behavior like sleep hygiene, caffeine intake, smoking habit or alcohol intake previously to the signal measuring procedure [18].

Regarding how the EEG activity can be related to an external stimulus that is affecting the subject, it can be considered as

- Spontaneous: generally treated as noise or basal EEG.

- Evoked: activity that can be detected synchronously after some specific amount of time after the onset of the stimulus. This is usually referred as time-locked. In contrast to the previous one, it is often called Induced activity.

Additionally, according to the existence of a repeated rhythm, the EEG activity can be understood as

- Rhythmic: EEG activity consisting in waves of approximately constant frequency. It is often abbreviated RA (regular rythmic activity). They are loosely classified by their frequencies, and their naming convention was derived from the original naming used by Hans Berger himself, and after Alpha Waves (10 Hz), it came Delta (4 Hz), Theta (4-7 Hz), Sigma (12-16 Hz), Beta (12-30 Hz) and Gamma (30-100 Hz).
- Arrhythmic: EEG activity in which no stable rhythms are present.
- Dysrhythmic: Rhythms and/or patterns of EEG activity that characteristically appear in patient groups and rarely seen in healthy subjects.

The number of electrodes and their positions over the scalp determines a **Spatial Structure**: signal elements can be generalized, focal or lateralized, depending on in which channel (i.e. electrode) they are found.

1.1. EEG Waveform Characterization

The shape of the signal, the waveform, can be defined as the graphed line that represents the signal's amplitude plotted against time. It can also be called EEG biomarker, EEG pattern, signal shape, signal form and a morphological signal [11].

The signal context is crucial for waveform characterization, both in a spatial and in a temporal domain [11]. Depending on the context, some specific waveform can be considered as noise while in other cases is precisely the element which has a cognitive functional implication.

A waveform can have a characteristic shape, a rising or falling phase, a pronounced plateau or it may be composed of ripples and wiggles. In order to describe them, they are characterized by its amplitude, the arch, whether they have (non)sinusoidal shape, by the presence of an oscillation or imitating a sawtooth (e.g. Motor Cortical Beta Oscillations). The characterization by their sharpness is also common, particularly in Epilepsy, and they can also be identified by their resemblance to spikes (e.g. Spike-wave discharge).

Depictions may include subjective definitions of sharper, arch comb or wicket shape, rectangular, containing a decay phase or voltage rise, peaks and troughs, short term voltage change around each extrema in the raw trace. Derived ratios and indexes can be used as well like peak and trough sharpness ratio, symmetry between rise and decay phase and slope ratio (steepness of the rise period to that of the adjacent decay period). For instance, wording like "Central trough is sharper and more negative that the adjacent troughs" [19] are common in the literature.

Other regular characterizations which are based on the waveform shape may encompass:

- Attenuation: Also called suppression or depression. Reduction of amplitude of EEG activity resulting from decreased voltage. When activity is attenuated by stimulation, it is said to have been "blocked" or to show "blocking".
- Hypersynchrony: Seen as an increase in voltage and regularity of rhythmic activity, or within the alpha, beta, or theta range. The term suggest an increase in the number of neural elements contributing to the rhythm, or in the synchronization of different neurons with the same discharge pattern [20].
- Paroxysmal: Activity that emerges from background with a rapid onset, reaching (usually) quite high voltage and ending with an abrupt return to lower voltage activity.
- Monomorphic: Activity appearing to be composed of one dominant waveform pattern.
- Polymorphic: Activity composed of multiple frequencies that combine to form a complex waveform.

151 • Transient: An isolated wave or pattern that is distinctly different from background activity.

152 The traditional clinical approach consists in analyzing the paper strip that is generated by
153 the plot of the signal obtained from the device. Expert technician and physicians analyze visually
154 the plots looking for specific patterns that may give a hint of the underlying cognitive process or
155 pathology. Atlases and guidelines were created in order to help in the recognition of these complex
156 patterns. Even Video-electroencephalography scalp recordings are routinely used as a diagnostic tools
157 [21] . The clinical EEG research has also focused on temporal waveforms, and a whole branch of
158 electrophenomenology has arisen around EEG *graphoelements* [5].

159 Sleep Research has been studied in this way by performing Polysomnographic recordings (PSG)
160 [22], where the different sleep stages are evaluated by visually marking waveforms or graphoelements
161 in long-running electroencephalographic recordings, looking for patterns based on standardized
162 guidelines. Visual characterization includes the identification or classification of certain waveform
163 components, or transient events, based on a subjective characterization (e.g. positive or negative peak
164 polarity) or the location within the strip. It is regular to establish an amplitude difference between
165 different waveforms from which a relation between them is established and a structured index are
166 created (e.g. sleep K-Complex is well characterized based on rates between positive vs negative
167 amplitude) [23]. Other relevant EEG patterns for sleep stage scoring are alpha, theta, and delta waves,
168 sleep spindles, polysplindles, vertex sharp waves (VSW), and sawtooth waves (REM Sleep).

169 Moreover, EEG data acquisition is a key procedure during the assessment of patients with
170 focal Epilepsy for potential seizure surgery, where the source of the seizure activity must be reliably
171 identified. The onset of the Epileptic Seizure is defined as the first electrical change seen in the EEG
172 rhythm which can be visually identified from the context and it is verified against any clinical sign
173 indicating seizure onset. The interictal epileptiform discharges (IEDs) are visually identified from the
174 paper strip, and they are also named according to their shape: spike, spike and wave or sharp-wave
175 discharges[24].

176 Waveform characterization is the method in which analysis has been performed for Event Related
177 Potentials. Evoked Potentials (EPs) and Event Related Potentials (ERPs) are transient signal elements
178 that may arise as a brain response to an external visual, tactile or auditory stimulus. Particularly,
179 ERPs are regularly used to assess auditory response in infants. They are extensively used and studied
180 in Cognitive Neuroscience [25]. ERPs are identified by their components which are recognizable
181 signal shapes assigned to the observed waveform, that can be linked to some cognitive or measurable
182 psychological process. The P300 is one of the most studied ERP component in BCI because it can
183 be used to implement a Speller application. Hence, P300 ERPs are a target phenomena to study by
184 automatic waveform recognition methods.

Table 1. EEG waveforms descriptions found in the surveyed literature.

Method	Phenomena	Reference
Positive Rounded Component	α-Waves, Epilepsy	[5,26]
Rising and Falling Phase	Epilepsy	[14,26]
Terminal plateau	Epilepsy	[14]
Ripples and Wiggles	Epilepsy, ERP	[14,24,27,28]
Sinusoidal Shape	Epilepsy	[19,26–29]
Sawtooth	Motor Imagery, Sleep	[22,24,26]
Sharpness or Spike-like	Epilepsy	[8,14,24,30]
Rectangular	Epilepsy	[14,19]
Wicket Shape	Epilepsy	[5,8,19,24,26,30]
Peak and Trough Sharpness Ratio	Epilepsy	[8,19,30,31]
Symmetry between rise and decay phase	Epilepsy	[8,19]
Slope Ratio	Sleep	[32]
Positive/Negative Peak Amplitude	ERP	[8,14,19,26,33,34]
Positive vs Negative Ratio	Sleep K-Complex	[24]
Base-to-Peak Amplitude	ERP	[19]
Peak-to-Peak Amplitude	ERP	[33]
Positive/Negative Peak Latency	ERP	[33]
Integrated Activity	ERP, Epilepsy,ICU	[23,35]
Cross-Correlation	ERP, Epilepsy, Sleep	[27,35]
Coupling		
Cross Frequency, Phase-Amplitude, Phase-Phase	Sleep	[19]
Period Amplitude Analysis	ERP, Epilepsy	[23,27,35]

2. Materials and Methods

The search of methods based on waveforms is conducted by following the PRISMA [36] guidelines. Search is performed on Google Scholar, Semantic Web and IEEE Xplore search engines by the terms "Waveforms" OR "Shape" OR "Morphology" OR "Visual inspection" + "EEG".

The following criteria is proposed to identify methods which are based on the signal's waveform:

1. The analysis consider the shape of the plot of the signal.
2. The pattern can be identified and verified by visual inspection.
3. The pattern matching is performed in time-domain.
4. The method encompass a feature extraction procedure.
5. The feature extraction procedure allows to create a template dictionary.

As described in [37] the Pattern Matching problem in Signal processing is finding a signal given the region that best describes the structure of the prototype signal template. On the other hand, a *feature* is a meaningful quantification, usually a multidimensional vector, that synthesize the information of a given signal or signal segment [38].

2.1. EEG Waveform Analysis Algorithms

Shape or waveform analysis methods are considered as nonparametric methods. They explore signal's time-domain metrics or even derive more complex indexes or features from it [39].

One of the earliest approach to automatically process EEG data is the Peak Picking method. Although of limited usability, peak picking has been used to determine latency of transient events in EEG [40,41]. Straightforward in its implementation, it consists in assigning a component to a simple waveform element based on the expected location of its more prominent deflection [29]. Of regular use in ERP Research, the name of many of the EEG features reference directly a peak within the component, e.g. P300 or P3a P3b or N100. This leads to a natural way to classify them visually by selecting appropriate peaks and matching their positions and amplitudes in an orderly manner. The letter provides the polarity (Positive or Negative) and the numbering shows the time referencing the stimulus onset, or the ordinal position of each peak (first, second, etc).

211 A related method is used in [42] where the area under the curve of the EEG is sumarized to
212 derive a feature. This was even used in the seminal work of Farwell and Donchin on P300 [38,43].
213 Additionally, a logarithmic graph of the peak-to-peak amplitude which is called amplitude integrated
214 EEG (aEEG) [35] is used nowadays in Neonatal Intensive Care Units.

215 Other works on EEG explored the idea to extend human capacities analyzing EEG waveforms
216 [44] where a feature derived from the amplitude and frequency of its signal and its derivative in
217 time-domain is used. Moreover, other approaches explored the use of Mathematical Morphology [45],
218 where the time-domain structure of contractions and dilations were studied. Finally the proposals
219 of Burch, Fujimori, Uchida and the Period Amplitude Analysis (PAA) [46] algorithm are few of the
220 earliest depictions where the idea of capturing the shape of the signal were established.

221 According to the defined criteria, the algorithms that will be evaluated are as follows:

222 • Matching Pursuit
223 • Permutation Entropy
224 • Slope Horizontal Chain Code
225 • Scale Invariant Feature Transform

226 All these methods provide a feature f that can be used as a template. The notation $\{\}_1^n$ will be
227 used to describe the concatenation of scalar values to form a multidimensional feature vector f. These
228 algorithms are based on metrics that are extracted from the shape of the single channel digital EEG
229 signal $x(n)$, with n varying from 1 to the length N of the EEG segment in sample points. These features
230 are used to create dictionaries or template databases. Finally, these templates provide the basis for the
231 pattern matching algorithm and offline classification. These algorithm were implemented on MATLAB
232 2014a (Mathworks Inc., Natick, MA, USA).

2.2. Matching Pursuit - MP 1 and MP 2

234 *Pursuit* algorithms refer, in their many variants, as blind source separation [47] techniques that
235 assume the EEG signal as a linear combination of different sparse sources extracted from a template's
236 dictionaries. Matching Pursuit *MP* [48], the most representative of this algorithms, is a greedy variant
237 that decomposes a signal into a linear combination of waveforms, called atoms, that are well localized
238 in time and frequency [49]. Given a signal, this optimization technique, tries to find the indexes of m
239 atoms and their weights (contributions) that minimize,

$$\varepsilon = \left\| x(n) - \sum_{i=1}^{m} w_i g_i(n) \right\| \tag{1}$$

240 which is the error between the signal and their approximation constructed by the weighted w_i atoms
241 g_i, and calculating the euclidean norm $\|\cdot\|_2$. The algorithm goes by first setting the approximating
242 signal $\tilde{x}_0$ as the original signal itself,

$$\tilde{x}_0(n) = x(n) \tag{2}$$

243 and setting the iterative counter k as 1. Hence, it searches recurrently the best template out of the
244 dictionary that matches current approximation.

$$g_k = \arg \max_{g_i} \left| \sum_{n=1}^{N} \tilde{x}_{k-1}(n) \, g_i(n) \right| \tag{3}$$

245 where g_i are all the available scaled, translated and modulated atoms from the dictionary. The operation
246 $|\cdot|$ corresponds to the absolute value of the inner product. This step determines the atom selection
247 process, and their contribution is calculated based on

$$w_k = \frac{\sum_{n=1}^{N} \tilde{x}_{k-1}(n) \, g_k(n)}{\|g_k\|^2} \tag{4}$$

with k representing the index of the selected atom g_k and $\|\cdot\|$ its norm. Finally the contribution of each atom is subtracted from the next approximation [30,48,50]

$$\tilde{x}_k(n) = \tilde{x}_{k-1}(n) - w_k g_k(n) \tag{5}$$

The stopping criteria can be established based on a limiting threshold on Equation 1 or based on a predetermined number of steps and selected atoms. Two variants of this algorithm are evaluated. In *MP 1* the dictionary is directly constructed with the normalized templates directly extracted from the real signal segments which is a straightforward implementation of the pattern matching technique. In *MP 2* the coefficients of Daubechies least-asymmetric wavelet with 2 vanishing moments atoms are used to construct the dictionary [51]. For the first version, the matching against the template is evaluated according to Equation 1 directly, whereas for the latter each feature is crafted by decomposing the signal in its coefficients and building, an eventually sparse, vector with them:

$$f = \left\{ w_i \right\}_1^D \tag{6}$$

where D is the size of the dictionary.

2.3. Permutation Entropy - PE

Bond and Pompe Permutation Entropy has been extensively used in EEG processing, with applications on Anesthesia, Sleep Stage evaluation and increasingly for Epilepsy pre-ictal detection [52]. This method generates a code based on the orderly arrangement of sequential samples, and then derives a metric which is based on the number of times each sequence is found on the signal. This numeric value can be calculated as information entropy [53]. Let's consider a signal on a window of length W represented by

$$(x_1, x_2, ..., x_W) \tag{7}$$

and resampled by τ intervals and starting from the sampling point n, doing

$$(x_n, x_{n+\tau}, x_{n+2\tau}..., x_{n+(m-1)\tau}) \tag{8}$$

This sequence is of order m, which is the number of sample points used to derive the ordinal element called π. There are $m!$ ways in which this sequence can be orderly arranged, according to the position that each sample point holds within the sequence in a strict order relationship. For example if $m = 3$, and the first sample point is the bigger, the second is the smaller and the third one is in the middle, the ordinal element π corresponds to $(3, 1, 2)$. Thus, along the signal window there can be at most k different ordinal (and overlapping) elements π_s

$$(\pi_1, \pi_2, ..., \pi_k) \tag{9}$$

with $k = W - (m - 1)\tau$. The probability density function *pdf* for all the available permutations of order m should be $\mathbf{p} = (p_1, p_2, ..., p_{m!})$ with $\sum_1^{m!} p_i = 1$.

Hence, the time series window is mapped to a new set of k ordinal elements, and the *pdf* can be calculated by the empirical permutation entropy,

$$p_i = \frac{1}{k} \sum_{s=1}^{k} [\pi_s = \pi_i] \tag{10}$$

with $1 \leq i \leq m!$. The Iverson Bracket $[\cdot]$ resolves to 1 when their logical proposition argument is true, 0 otherwise. Therefore, for each i only those ordinal elements π_s that were effectively found along

the signal are counted to estimate p_i, and zero elsewhere. The empirical permutation entropy can be estimated from this histogram as,

$$H(\mathbf{p}) = \sum_{i=1}^{m!} p_i \, log \, \frac{1}{p_i}. \tag{11}$$

The implemented code was derived from [54], and the model description from [55]. This procedure will produce a scalar number for the given signal window of size W. To derive a feature, a sliding window procedure must be implemented. Thus, the length of the feature is $N - (W + \tau(m-1)) + 1$.

$$f = \left\{ H(\mathbf{p})_u \right\}_1^{N-(W+\tau(m-1))+1} \tag{12}$$

with u varying on a sample by sample basis along the signal but excluding the first window.

2.4. Slope Horizontal Chain Code - SHCC

This method is an extension of Slope Chain Code (SCC) [42]. This algorithm proceeds by generating a coding scheme from a sequence of sample points. This encoding is based on the angle between the horizontal line on a 2D-plane and any segment produced by two consecutive sample points, regarding them as coordinates on that plane.

A signal of length N, can be represented by a list of ordered-pairs e,

$$e = [(x,y)_1, (x,y)_2, ..., (x,y)_N] \tag{13}$$

and it can be divided into G different blocks. These blocks are obtained by resampling the original signal from the index

$$G = \lfloor n + (m\Delta) + 0.5 \rfloor \tag{14}$$

with n being the original sampling index on $1 \le n \le N$ and $\lfloor \cdot \rfloor$ being the floor operation, i.e. rounding of the number argument to the closest smaller integer number. On the other hand, Δ can be obtained by

$$\Delta = \left\lceil \frac{N}{G+1} \right\rceil \tag{15}$$

with $G < N$ and using instead $\lceil \cdot \rceil$ as the ceil operation, the rounding to the closest bigger integer number. Lastly, the value m can be derived from

$$m = sign\left(\frac{N-1}{\Delta}\right) \left\lfloor \left| \frac{N-1}{\Delta} \right| \right\rfloor \tag{16}$$

This resampling produces a new sequence of values,

$$e = \left[(x',y')_1, ..., (x',y')_s, ..., (x',y')_G \right] \tag{17}$$

The next step is the normalization of each ordered-pair as vectors $\mathbf{x}' = (x'_1, ..., x'_G)$ and $\mathbf{y}' = (y'_1, ..., y'_G)$ according to

$$\hat{\mathbf{x}} = \frac{(\mathbf{x}' - \min(\mathbf{x}')\mathbf{1})}{\max(\mathbf{x}') - \min(\mathbf{x}')} \tag{18}$$

$$\hat{\mathbf{y}} = \frac{(\mathbf{y}' - \min(\mathbf{y}')\mathbf{1})}{\max(\mathbf{y}') - \min(\mathbf{y}')} \tag{19}$$

302 with **1** being the vector of length G with all their components equal to 1. This operation effectively
303 normalize the components $\hat{x}_s, \hat{y}_s \in [0, 1]$.

304

305 Finally, the feature is constructed by calculating the point-to-point slope against the horizontal
306 plane,

$$f = \left\{ \frac{\hat{y}_s - \hat{y}_{s-1}}{\hat{x}_s - \hat{x}_{s-1}} \right\}_2^G \tag{20}$$

307 *2.5. Scale Invariant Feature Transform - SIFT*

308 SIFT [56] is a very successful feature extraction technique from Computer Vision . It has a
309 biomimetic inspiration on how the visual cortex analyze images based on orientations [57]. This
310 method has been used in [58] to analyze EEG signals based on their plots on 2D images.
311 The first step of the algorithm is the plot generation based on single-channel EEG segments $x(n)$.
312 Hence, this signal is normalized by the z-score [59]:

$$\tilde{x}(n) = \left\lfloor \frac{\delta(x(n) - \bar{x})}{\sigma_x} \right\rfloor \tag{21}$$

313 with δ being the signal magnification factor and $\bar{x}$ and σ_x, the mean and standard deviation of x on
314 the signal segment. The width of the image is determined based on the 1-second length size of the
315 segment window in sample units. This corresponds to the sampling frequency F_s of the EEG signal
316 segment. The width is adjusted by multiplying by the magnification factor δ,

$$w = \delta \, F_s \tag{22}$$

317 whereas the height is calculated based on the peak-to-peak amplitude of the signal within the segment,

$$h = \left(\max_n \tilde{x}(n) - \min_n \tilde{x}(n) \right). \tag{23}$$

318 Equation 24 determines the vertical position of the image where the signal's zero value will be
319 located.

$$z = \left\lfloor \frac{h}{2} \right\rfloor - \left\lfloor \frac{\max_n \tilde{x}(n) + \min_n \tilde{x}(n)}{2} \right\rfloor \tag{24}$$

320 Finally, a binary, black-and-white image plot is generated based on

$$I(z_1, z_2) = \begin{cases} 255 & \text{if } z_1 = \delta \, n; z_2 = \tilde{x}(n) + z \\ 0 & \text{otherwise} \end{cases} \tag{25}$$

321 where z_1 and z_2 are the image coordinates values. These points are interpolated using the Bresenham
322 algorithm.
323 Once the plot is generated, the plot's center is used to localize the center of the SIFT patch.
324 This region of the image, where the signal's most important salient waveform should be located, is
325 divided in a grid of $4x4$ block and the bidimensional gradient vectors are calculated on each one of
326 them. Therefore, for each block within the patch, a histogram of the gradient orientations, 8 circular
327 orientations, are calculated. This histogram is concatenated for all the 16 blocks and a feature is thus
328 formed:

$$f = \left\{ h(i, j, \theta) \right\}_{(0,0,0)}^{(3,3,315)} \tag{26}$$

with *i* and *j* varying between 0 and 3, localizing the 16 blocks within the grid. The angles θ are the eight possible equidistant values between 0 and 315. This vector is normalized, clamped to 0.2, and re-normalized again. Details of the method can be found on [56,58]. It was implemented using the VLFeat [60] public Computer Vision libraries.

2.6. Experimental Protocol

Farwell and Donchin P300 Speller [43] is one the most used BCI paradigms to implement a thought translation device and to send commands to a computer in the form of selected letters, similar to typing in a virtual keyboard. This procedure exploits a cognitive phenomena raised by the oddball paradigm: along the EEG trace of a person which is focusing on a sequence of two different visual flashing stimulus, a particular and distinctive transient component is found each time the expected stimulus flashes. This is cleverly utilized in the P300 Speller, where rows and columns of a 6x6 matrix flashes randomly but only the flashing of a column or row where the letter that a user is focusing will trigger concurrently the P300 ERP along the EEG trace.

How much is it possible to classify and implement a P300 ERP Speller using only the waveform structure of the signal ? Which algorithm perform better at this even when segment latency variations and component amplitudes issues are present ?

In order to verify this in a controlled procedure, a real P300 ERP template, obtained from a public dataset, is superimposed into a different EEG stream. This trace was experimentally obtained by a subject which was observing the flashing of the stimulus matrix during a P300 Speller procedure but did not engage in focusing on any letter in particular. Everything is there, except the P300 ERP component. By implementing this pseudo-real approach, it is possible to effectively control null-signals and to adjust the shape of this evoked potential in accordance to similar procedures used in other works [29,40,61].

The experiments are as follows:

- Experiment 1 - Pseudo-Real Dataset Classification Performance: the letter classification performance of each one of these methods applied on the artificially generated pseudo-real dataset.
- Experiment 2 - Latency Noise: Uniform noise is added to the ERP template latency, i.e. the temporal location where it is injected into the EEG stream. The latency range from 0 to 40% of the 1*s* of the window size.
- Experiment 3 - Component Amplitude Noise: the amplitude of the main P3b components of the ERP template is altered based on uniform distribution. This component is completely substracted from the original template or not substracted at all. The substraction percentage is obtained from a uniform distribution. Additionally the substraction curve is warped in a gaussian window of 800 ms.

2.6.1. Pseudo-Real Dataset Generation

The template ERP is extracted from the Subject Number 8 of the public dataset 008-2014 [62] published on the BNCI-Horizon website [63] by IRCCS Fondazione Santa Lucia. Segments from the EEG signal are labeled as hit and are extracted for the trial number 2, and they are point-to-point coherently averaged. This P300 ERP can be seen in Fig. 2.

An EEG stream with null-P300 signal is obtained by the following procedure: A subject participant is recruited voluntarily and the experiment is conducted anonymously in accordance with the Declaration of Helsinki published by the World Health Organization. No monetary compensation is handed out and she/he agrees and signs a written informed consent. This study is approved by the *Departamento de Investigación y Doctorado, Instituto Tecnológico de Buenos Aires (ITBA)*. The participant is healthy and have normal or corrected-to-normal vision and no history of neurological disorders. This voluntary subject is aged between 20-30 years old. EEG data is collected in a single recording session. She/He is seated in a comfortable chair, with her/his vision aligned to a computer screen located

one meter in front of her/him. The handling and processing of the data and stimuli is conducted by the OpenVibe platform [64]. Gel-based active electrodes (g.LADYbird, g.Tec, Austria) are used on locations Fz, Cz, Pz, Oz, P3,P4, PO7 and PO8 according to the 10-20 international system. Reference is set to the right ear lobe and ground is preset as the AFz position. Sampling frequency is set to 250 Hz.

The participant is instructed to passively watch the flashing screen while not focusing on any particular letter. A questionnaire is handed out at the end of the experiment with questions about how the participant felt during it, without giving more details.

Fig. 3 shows a 5*s* sample of the EEG trace. Channel *S* represents the twelve different stimulus markers (columns or rows) while channel *L* represent the label (hit vs nohit). Nohit are marked as a square signal and hit are markers are identified by the double-amplitude square signals. Subfigure (a) shows the signals before the ERP template is superimposed while subfigure (b) shows the same signals with the superimposed ERP template. At first sight differences are really hard to spot visually. Subfigures (c) and (d) show only one second of the same segment only channel Cz and Label. The superimposed ERP can be divised around 31.5s where in (d) the peak is bigger. Fig. 4 shows the obtained ensemble average ERPs as result of superimposing the template signal into EEG stream, time-locked to the stimulus onset. These 12 point-to-point averaged segments correspond to the first trial of the EEG stream.
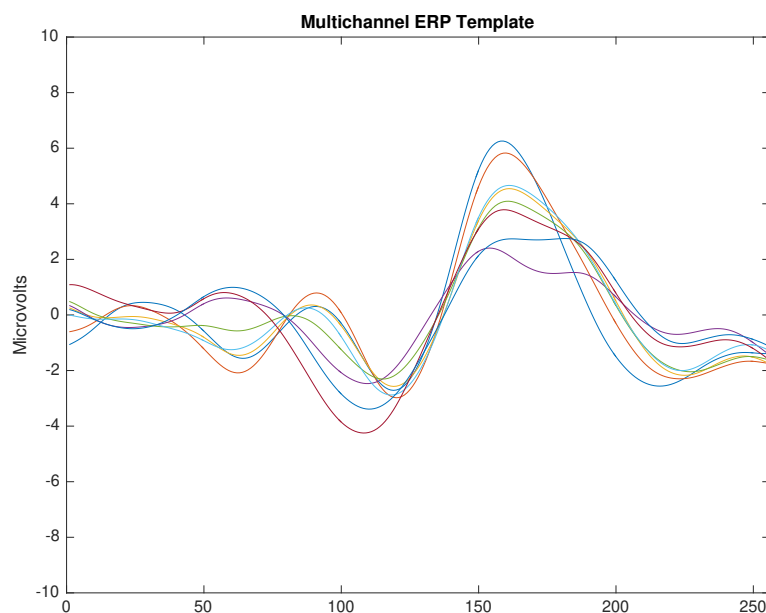

Figure 2. ERP Template obtained from the coherent point-to-point ensemble average of subject Eight obtained from the BNCI Horizon public dataset 008-2014. The template is 1*s* long which is 256 sample points, and the eight channels are superimposed with different colors. The P1, N1 and P300 peaks can be seen.
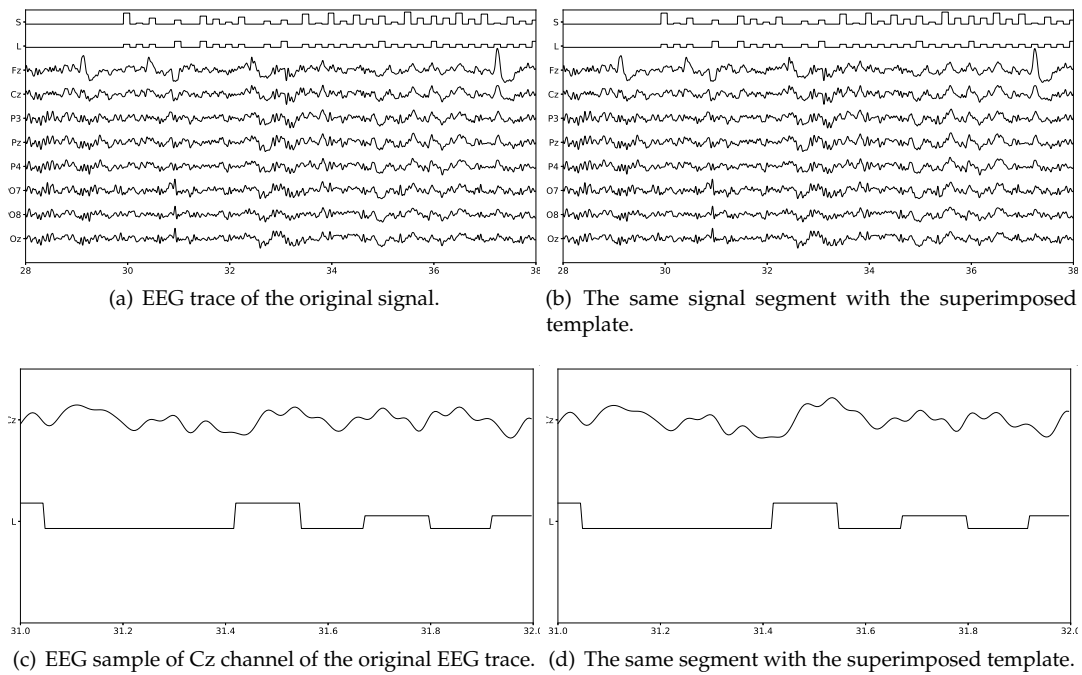
(a) EEG trace of the original signal.

(b) The same signal segment with the superimposed template.

(c) EEG sample of Cz channel of the original EEG trace. (d) The same segment with the superimposed template.

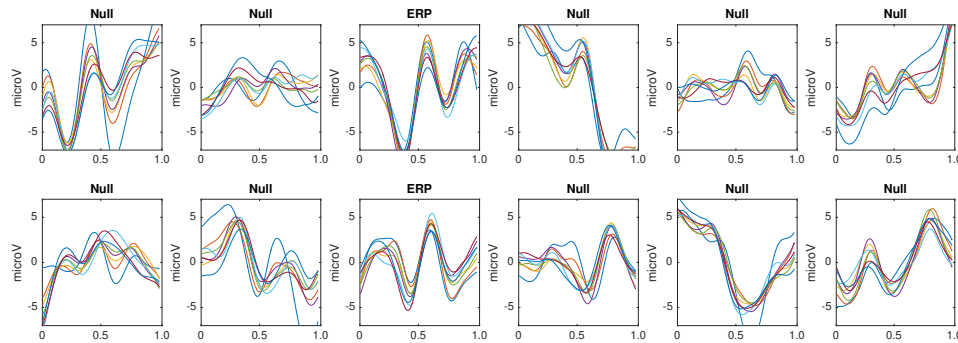**Figure 3.** Eight-channel EEG signal superimposed with the ERP Template.

Figure 4. Point-to-point averaged signals for the first letter identification trial. The ERP was superimposed on classes 3 and 9. Class 3 was obtained while averaging the segments where the row of the speller matrix was intensified whereas class 9 was calculated from the intensification of the corresponding column.

2.6.2. Classification

The same classification algorithm based on k-nearest neighbors is used for all the methods [65]. The experiment is composed of 35 trials to spell 7 words of 5 letters each. Each trial is composed of 10 intensification sequences of the 6 columns and 6 rows of the Speller Matrix. The first 15 trials are used to build the dictionary of templates, extracting the EEG segment for the row and column that contain the P300 ERP, hence shielding 30 different templates (Fig. 5).

Described algorithms produce a feature f for each EEG segment. The aim of the classification procedure is to identify for the remaining 20 trials which of the 6 features f that were obtained for row intensification and which of the 6 features for column intensifications are the ones that elicited the P300 response on the averaged EEG segment. The row number of the matrix can be obtained by doing

$$r\hat{o}w = \arg \min_{u \in \{1,\dots,6\}} \sum_{q_i=1}^{k} \|f_u - q_i\|^2 \tag{27}$$

with q_i being the set of k-nearest neighbors of the feature f_u with u varying from 1 to 6. The parameter k represents the number of neighbors chosen from the dictionary of templates. The column can be obtained by the same way,

$$c\hat{o}l = \arg \min_{u \in \{7,\dots,12\}} \sum_{q_i=1}^{k} \|f_u - q_i\|^2 . \tag{28}$$

Thus, the letter identification performance can be obtained by measuring the accuracy at identifying the correct letter on the matrix, coordinated by $r\hat{o}w$ and $c\hat{o}l$.
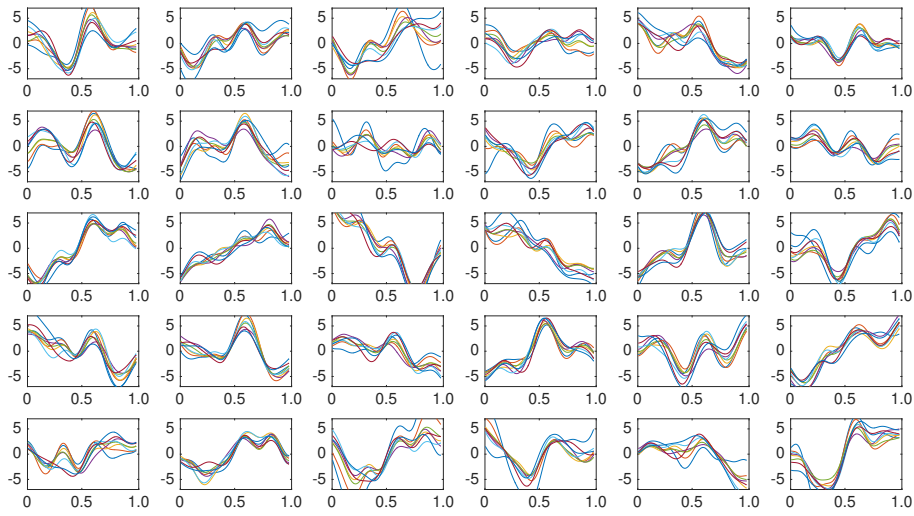

Figure 5. Coherently averaged signals containing the superimposed ERP. Each one is extracted from the 15 first trials (2 signals from each trial, one belonging to the column flashing and the other to row flashing). These are the templates used to build the dictionary and that are used by the classification algorithm described in 2.6.2.

Finallly, the classification method Support Vector Machine SVM is added for comparison as control using a feature f constructed by normalizing the signal on each channel [66]. This method is bla bla bla due to the reason bla bla bla.

3. Results

Results are shown in Table 2 and in Figure 6,7 and 8. Table 2 shows the single-intensification performance while identifying each letter of the standard P300 Speller Matrix, and the channel where the best performance was attained. Figure 6 shows the performance curves for eight algorithms. Each one represents the percentage of letters that were actually predicted by the combination of feature plus a classification method. As previously described the data were divided in two, and the first 15 letters were used to derive the dictionary of templates while the remaining 20 letters were used to measure the classification performance. Figure 7 shows the same results obtained when the ERP was superimposed with a noisy latency shift. Finally, Figure 8 represents the performance values obtained when the amplitude of the P3b component of the template are randomly attenuated.

Table 2. Speller classification performance obtained for all the waveform-based algorithms: MP Matching Pursuit, SIFT Scale Invariant Feature Transform, PE Permutation Entropy and SHCC Slope Horizontal Code Chain. Additionally, the control algorithms SVM Support Vector Machines was included, with a linear kernel. All the methods process the signal on a channel-by-channel basis, hence the best performing channel is also shown. In this case with absence of null-signals, it can be interpreted as the channel that adds less noise to the ERP template. All the methods used 10 intensification sequences to coherently average the trials to obtain the averaged signal.

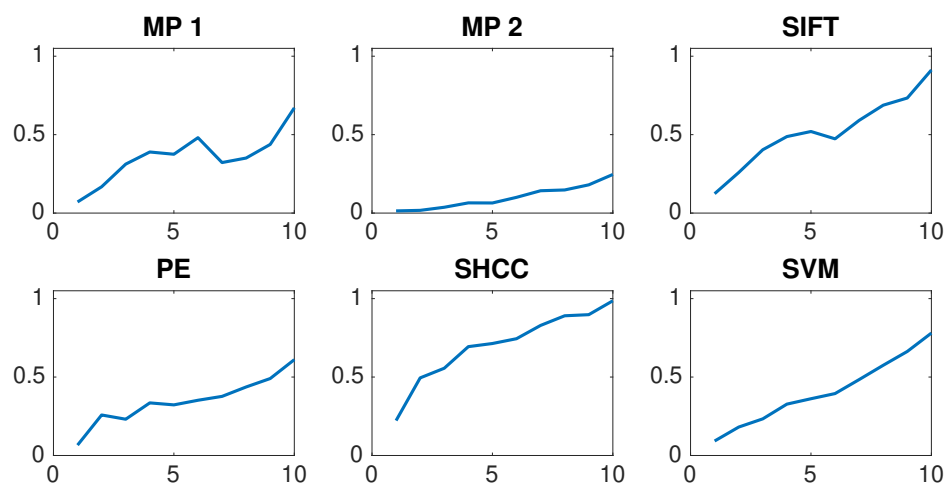| Method	Channel	Performance	Perf w/Latency noise	Perf w/Amplitude Noise
MP 1	PO8	67%	15%	50%
MP 2	PO7	24%	6%	10%
SIFT	PO8	91%	18%	66%
PE	Cz	61%	9%	32%
SHCC	P4	98%	31%	80%
SVM	PO8	78%	7%	53%

Figure 6. Speller performance obtained for each method. Y-axis shows performance accuracy while X-axis shows the number of intensification sequences used to calculate the point-to-point signal average.
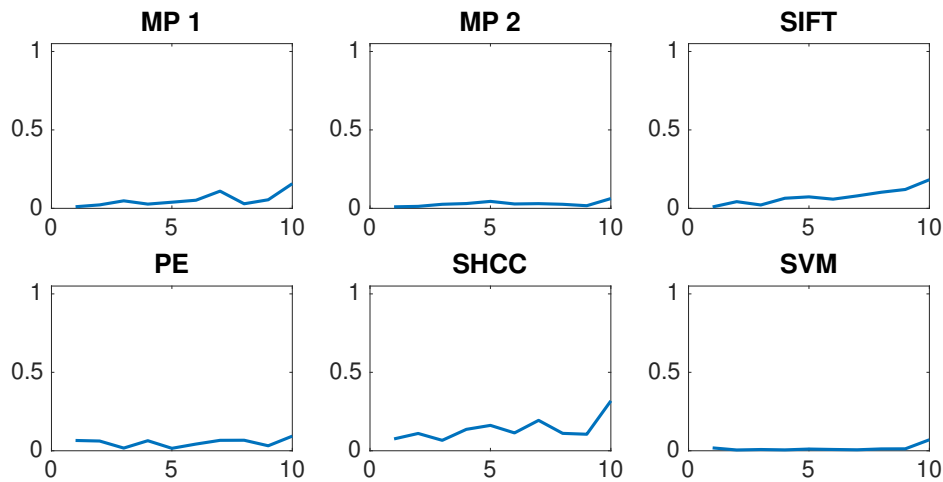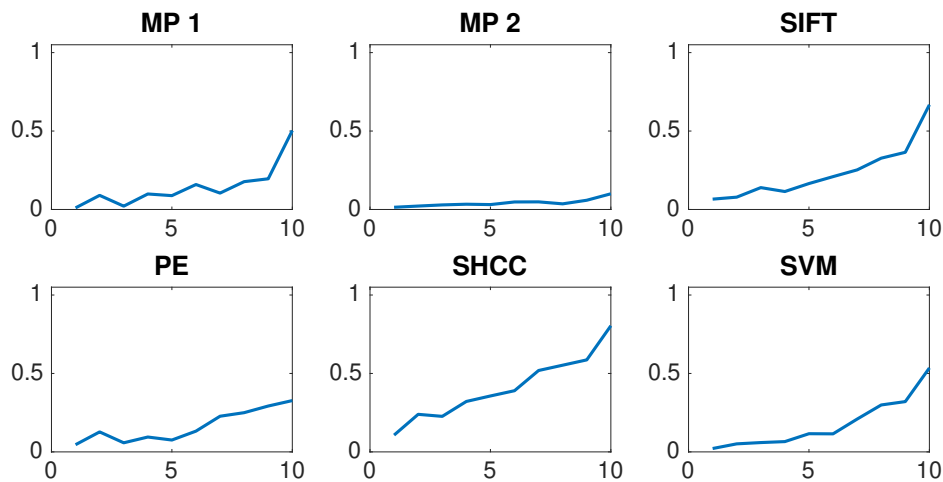
Figure 7. Speller performance obtained for each method while latencies were artificially added to each single-intensification segment. The achieved performance is significantly reduced for all methods. Y-axis shows performance accuracy while X-axis shows the number of intensification sequences used to calculate the point-to-point signal average.

Figure 8. Speller performance obtained while the amplitudes of the N1 and P3 component of the superimposed ERP are randomly reduced. Y-axis shows performance accuracy while X-axis shows the number of intensification sequences used to calculate the point-to-point signal average.

4. Discussion

All the methods show a significant reduction of performance when latency noise is added, and at the same time all the methods show some resistance to noise in peak amplitudes of the main components.

Using a straightforward dictionary of templates for *MP-1* proved more beneficial in terms of performance than the standard approach of using a Hilbert base of Wavelets atoms on *MP-2*. Either applying latency noise or amplitude noise, the method based on the signal's templates instead of using their coefficient proved to achieve much better performance values.

Results obtained for algorithms MP-1, SIFT, SHCC show them to be comparable with the results obtained for SVM. Particularly, the methods *SIFT* and *SHCC* performed much better than the other algorithms even when the latency and the amplitudes are noisy. Latency noise on the other hand,

reduces the information contained in the signal, mainly due to the invalidation of the SNR enhancement performed by the averaging procedure. This reduction impacts on the obtained performance for all the methods, almost equally.

5. Conclusion

The purpose of this work was threefold, (1) raise awareness about the utility of using automatic waveform-based methods to study EEG signals, (2) to provide an overview of the state-of-the-art of those methods, and (3) to compare those methods and verify if it is possible to obtain acceptable classification accuracies based exclusively on the signal's waveform.

We verified that similar performance results are obtained for the methods *MP-1*, *SIFT* and *SHCC* and that it is possible to obtain discriminating information from the underlying signal based exclusively on an automated method of processing the waveforms. This open the possibility to use these techniques to implement automatic detection procedures with a strong intelligible property, due to the fact that they are based on metrics which can be visually verified.

One of the main goals of the BCI discipline is to provide assistance to patients and to provide alternative tools to be used in diagnostics and rehabilitation procedure. This requires a clinical focus which is often neglected in BCI research [67]. At the same time, BCI reliability is yet an unfulfilled goal in this discipline [38]. The benefits of analyzing or including metrics about the shape of the EEG, are that clinical EEG diagnosis may support a vast set of already understood knowledge which is based on identifying EEG patterns by their shape and that can lead to more robust implementation of BCI devices.

The conventional clinical method of observing the waveform is understood to be subjective and laborious because results depend on the technicians' experience and expertise. The need for more objective measurements pushed the adoption of more automated means of decoding the signals and demanded a need for replication [14]. This lead to the initial development of quantitative EEG, which however didn't replaced clinically the traditional approach which is still widespread: the Gold standard in clinical EEG is still *Eye Ball*. We believe that the adoption of *hybrid* methodology which can process the signal automatically, but at the same time, maintains an intelligible property that can be mapped to existing procedures, and above all, can mantain the clinician control of the procedure will be beneficial to clinical practice, Neuroscience and BCI research.

These methods have the advantage that they can map a visual component with a clinical meaning to feature with a clear mathematical representation. Successful approaches in Computer Vision and Pattern Recognition in other areas use an ensemble of features to compound classifiers [68], with a significant enhancement of the classification performances [69].

Another benefit of these approaches is that they have a potential universal applicability. As they are only analyzing waveform, they can be explored in other disciplines where the structure or shape of the waveform is of relevance. Analyzing signals by their waveforms is relative common in chemical analysis [70], seismic analysis in Geology [71], and quantitative financial analysis. Electrocardiogram EKG, on the other hand, has been extensively processed and studied analyzing the waveform structure [72].

Author Contributions: This projects is part of a the first author's PhD Thesis which is directed by Juan Miguel Santos and codirected by Ana Julia Villar.

Abbreviations

The following abbreviations are used in this manuscript:

EEG: electroencephalography

BCI: Brain Computer Interfaces

BMI: Brain Machine Interfaces

BNCI: Brain-Neural Computer Interfaces

SNR: Signal to Noise Ratio

CNS: Central Nervous System

DC: Direct Current

ERP: Event-Related Potential

P300: Positive deflection of an Event-Related Potential which occurs 300 ms after onset of stimulus

ITR: Information Transfer Rate

BTR: Bit Transfer Rate

SIFT: Scale Invariant Feature Transform

SHCC: Slope Horizontal Chain Code

PE: Permutation Entropy

MP: Matching Pursuit

ICU: Intensive Care Unit

EKG: Electrocardiogram

PAA:Period Amplitude Analysis

1. Wolpaw, J.R.; Birbaumer, N.; McFarland, D.J.; Pfurtscheller, G.; Vaughan, T.M. Brain-computer interfaces for communication and control. *Clinical neurophysiology : official journal of the International Federation of Clinical Neurophysiology* **2002**, *113*, 767–91.

2. Lutz, W.; Sanderson, W.; Scherbov, S. The coming acceleration of global population ageing. *Nature* **2008**, *451*, 716–719.

3. Domingo, M.C. An overview of the Internet of Things for people with disabilities. *Journal of Network and Computer Applications* **2012**, *35*, 584–596.

4. Guger, C.; Allison, B.Z.; Lebedev, M.A. Introduction. In *Brain Computer Interface Research: A State of the Art Summary 6*; Springer, Cham, 2017; pp. 1–8.

5. Schomer, D.L.; Silva, F.L.D. *Niedermeyer's Electroencephalography: Basic Principles, Clinical Applications, and Related Fields*; Walters Klutter -Lippincott Williams & Wilkins, 2010.

6. Puce, A.; Hämäläinen, M.S. A review of issues related to data acquisition and analysis in EEG/MEG studies. *Brain Sciences* **2017**, *7*.

7. De Vos, M.; Debener, S. Mobile eeg: Towards brain activity monitoring during natural action and cognition. *International Journal of Psychophysiology* **2014**, *91*, 1–2.

8. Hartman, a.L. *Atlas of EEG Patterns*; Vol. 65, 2005; pp. E6–E6.

9. Yuste, R.; Goering, S.; Agüeray Arcas, B.; Bi, G.; Carmena, J.M.; Carter, A.; Fins, J.J.; Friesen, P.; Gallant, J.; Huggins, J.E.; Illes, J.; Kellmeyer, P.; Klein, E.; Marblestone, A.; Mitchell, C.; Parens, E.; Pham, M.; Rubel, A.; Sadato, N.; Sullivan, L.S.; Teicher, M.; Wasserman, D.; Wexler, A.; Whittaker, M.; Wolpaw, J. Four ethical priorities for neurotechnologies and AI. *Nature* **2017**, *551*, 159–163.

10. Jestico, J.; Fitch, P.; Gilliatt, R.W.; Willison, R.G. Automatic and rapid visual analysis of sleep stages and epileptic activity. A preliminary report. *Electroencephalography and Clinical Neurophysiology* **1977**, *43*, 438–441.

11. Jansen, B.H. Quantitative analysis of electroencephalograms: is there chaos in the future? *International Journal of Bio-Medical Computing* **1991**, *27*, 95–123.

12. Nijboer, F.; Broermann, U. Brain–Computer Interfaces for Communication and Control in Locked-in Patients; Springer Berlin Heidelberg, 2009; pp. 185–201.

13. Wei, Z.C.; Zou, J.Z.; Zhang, J.; Chen, L.L. Automatic recognition of epileptic discharges based on shape similarity in time-domain. *Biomedical Signal Processing and Control* **2017**, *33*, 236–244.

14. Thakor, N.V.; Tong, S. Advances in Quantitative Electroencephalogram Analysis Methods. *Annual Review of Biomedical Engineering* **2004**, *6*, 453–495.

15. Jackson, A.F.; Bolger, D.J. The neurophysiological bases of EEG and EEG measurement: A review for the rest of us. *Psychophysiology* **2014**, *51*, 1061–1071, [https://onlinelibrary.wiley.com/doi/pdf/10.1111/psyp.12283].

16. Haberman, M.A.; Spinelli, E.M. A multichannel EEG acquisition scheme based on single ended amplifiers and digital DRL. *IEEE Transactions on Biomedical Circuits and Systems* **2012**, *6*, 614–618.

17. Weeda, W.D.; Grasman, R.P.P.P.; Waldorp, L.J.; van de Laar, M.C.; van der Molen, M.W.; Huizenga, H.M. A fast and reliable method for simultaneous waveform, amplitude and latency estimation of single-trial EEG/MEG data. *PLoS ONE* **2012**, *7*.

18. Farzan, F.; Atluri, S.; Frehlich, M.; Dhami, P.; Kleffner, K.; Price, R.; Lam, R.W.; Frey, B.N.; Milev, R.; Ravindran, A.; McAndrews, M.P.; Wong, W.; Blumberger, D.; Daskalakis, Z.J.; Vila-Rodriguez, F.; Alonso, E.; Brenner, C.A.; Liotti, M.; Dharsee, M.; Arnott, S.R.; Evans, K.R.; Rotzinger, S.; Kennedy, S.H. Standardization of electroencephalography for multi-site, multi-platform and multi-investigator studies: Insights from the canadian biomarker integration network in depression. *Scientific Reports* **2017**, *7*, 7473.

19. Cole, S.R.; Voytek, B. Brain Oscillations and the Importance of Waveform Shape. *Trends in Cognitive Sciences* **2017**, *21*, 137–149.

20. Buzsáki, G.; Anastassiou, C.A.; Koch, C. The origin of extracellular fields and currents-EEG, ECoG, LFP and spikes. *Nature Reviews Neuroscience* **2012**, *13*, 407–420, [NIHMS150003].

21. Giagante, B.; Oddo, S.; Silva, W.; Consalvo, D.; Centurion, E.; D'Alessio, L.; Solis, P.; Salgado, P.; Seoane, E.; Saidon, P.; Kochen, S. Clinical-electroencephalogram patterns at seizure onset in patients with hippocampal sclerosis. *Clinical Neurophysiology* **2003**, *114*, 2286–2293.

22. Rodenbeck, A.; Binder, R.; Geisler, P.; Danker-Hopfe, H.; Lund, R.; Raschke, F.; Weeß, H.G.; Schulz, H. A review of sleep EEG patterns. Part I: A compilation of amended rules for their visual recognition according to Rechtschaffen and Kales. *Somnologie* **2006**, *10*, 159–175.

23. Uchida, S.; Feinberg, I.; March, J.D.; Atsumi, Y.; Maloney, T. A comparison of period amplitude analysis and FFT power spectral analysis of all-night human sleep EEG. *Physiology and Behavior* **1999**, *67*, 121–131.

24. Britton, J.W.; Frey, L.C.; Hopp, J.L.; Korb, P.; Koubeissi, M.Z.; Lievens, W.E.; Pestana-Knight, E.M.; St. Louis, E.K. Electroencephalography (EEG): An Introductory Text and Atlas of Normal and Abnormal Findings in Adults, Children, and Infants, 2016.

25. Luck, S.J. *An Introduction to the Event-Related Potential Technique*; Vol. 78, 2005; p. 388, [9780262621960].

26. Tatum, W.; Husain, A.; Benbadis, S.; Kaplan, P. *Handbook of EEG Interpretation*; Demos Medical Publishing, 2008.

27. Cacioppo, J.; Tassinary, L.G.; Berntson, G.G. *The Handbook of Psychophysiology*; 2007; [arXiv:1011.1669v3].

28. Kappenman, E.S.; Luck, S.J. *The Oxford Handbook of Event-Related Potential Components*; 2012; [arXiv:1011.1669v3].

29. Ouyang, G.; Hildebrandt, A.; Sommer, W.; Zhou, C. Exploiting the intra-subject latency variability from single-trial event-related potentials in the P3 time range: A review and comparative evaluation of methods. *Neuroscience and Biobehavioral Reviews* **2017**, *75*, 1–21.

30. Sanei, S.; Chambers, J. *EEG Signal Processing*; 2007; [arXiv:1011.1669v3].

31. Hirsch, L.J.; Richard, B.P. *Atlas of EEG in critical care*; Wiley-Blackwell, 2010; p. 348, [arXiv:1011.1669v3].

32. Subha, D.P.; Joseph, P.K.; Acharya U, R.; Lim, C.M. EEG signal analysis: a survey. *Journal of medical systems* **2010**, *34*, 195–212.

33. Mak, J.N.; McFarland, D.J.; Vaughan, T.M.; McCane, L.M.; Tsui, P.Z.; Zeitlin, D.J.; Sellers, E.W.; Wolpaw, J.R. EEG correlates of P300-based brain-computer interface (BCI) performance in people with amyotrophic lateral sclerosis. *Journal of Neural Engineering* **2012**, *9*.

34. Müller-Putz, G.R.; Riedl, R.; Wriessnegger, S.C. Electroencephalography (EEG) as a research tool in the information systems discipline: Foundations, measurement, and applications. *Communications of the Association for Information Systems* **2015**, *37*, 911–948.

35. Shah, N.A.; Wusthoff, C.J. How to use: Amplitude-integrated EEG (aEEG). *Archives of Disease in Childhood: Education and Practice Edition* **2015**, *100*, 75–81.

36. Moher, D.; Liberati, A.; Tetzlaff, J.; Altman, D.G.; Altman, D.; Antes, G.; Atkins, D.; Barbour, V.; Barrowman, N.; Berlin, J.A.; Clark, J.; Clarke, M.; Cook, D.; D'Amico, R.; Deeks, J.J.; Devereaux, P.J.; Dickersin, K.; Egger, M.; Ernst, E.; Gøtzsche, P.C.; Grimshaw, J.; Guyatt, G.; Higgins, J.; Ioannidis, J.P.; Kleijnen, J.; Lang, T.; Magrini, N.; McNamee, D.; Moja, L.; Mulrow, C.; Napoli, M.; Oxman, A.; Pham, B.; Rennie, D.; Sampson,

M.; Schulz, K.F.; Shekelle, P.G.; Tovey, D.; Tugwell, P. Preferred reporting items for systematic reviews and meta-analyses: The PRISMA statement. *PLoS Medicine* **2009**, *6*, e1000097, [arXiv:1011.1669v3].

37. Allen, R.L.; Mills, D. *Signal analysis: time, frequency, scale, and structure*; John Wiley & Sons, 2004.

38. Wolpaw, Jonathan R, W.E. *Brain-Computer Interfaces: Principles and Practice*; Oxford University Press, 2012; p. 400.

39. Thakor, N. *Quantitative EEG analysis methods and clinical applications*; 2009; p. 440.

40. Jaškowski, P.; Verleger, R. An evaluation of methods for single-trial estimation of P3 latency. *Psychophysiology* **2000**, *37*, 153–162.

41. Zhang, D.; Luo, Y. The P1 latency of single-trial ERPs estimated by two peak-picking strategies. *Proceedings - 2011 4th International Conference on Biomedical Engineering and Informatics, BMEI 2011* **2011**, *2*, 882–886.

42. Alvarado-González, M.; Garduño, E.; Bribiesca, E.; Yáñez-Suárez, O.; Medina-Bañuelos, V. P300 Detection Based on EEG Shape Features. *Computational and Mathematical Methods in Medicine* **2016**, *2016*, 1–14.

43. Farwell, L.A.; Donchin, E. Talking off the top of your head: toward a mental prosthesis utilizing event-related brain potentials. *Electroencephalography and Clinical Neurophysiology* **1988**, *70*, 510–523.

44. F.F., K. A waveform analyzer applied to the human EEG. *IEEE Transactions on Biomedical Engineering* **1976**, *23*, 246–252.

45. Yamaguchi, T.; Fujio, M.; Inoue, K.; Pfurtscheller, G. Design Method of Morphological Structural Function for Pattern Recognition of EEG Signals During Motor Imagery and Cognition. 2009 Fourth International Conference on Innovative Computing, Information and Control (ICICIC). IEEE, 2009, pp. 1558–1561.

46. Uchida, S.; Matsuura, M.; Ogata, S.; Yamamoto, T.; Aikawa, N. Computerization of Fujimori's method of waveform recognition a review and methodological considerations for its application to all-night sleep EEG. *Journal of Neuroscience Methods* **1996**, *64*, 1–12.

47. Vincent, E.; Deville, Y. *Handbook of Blind Source Separation - Independent Component Analysis and Applications*; Elsevier, 2010; p. 831.

48. Mallat, S.G.; Zhang, Z. Matching Pursuits With Time-Frequency Dictionaries. *IEEE Transactions on Signal Processing* **1993**, *41*, 3397–3415.

49. Chandran KS, S.; Mishra, A.; Shirhatti, V.; Ray, S. Comparison of Matching Pursuit Algorithm with Other Signal Processing Techniques for Computation of the Time-Frequency Power Spectrum of Brain Signals. *Journal of Neuroscience* **2016**, *36*, 3399–3408.

50. Cohen, M.X. *Analyzing Neural Time Series Data: Theory and Practice*; 2014; [arXiv:1011.1669v3].

51. Vařeka, L. Matching pursuit for p300-based brain-computer interfaces. *2012 35th International Conference on Telecommunications and Signal Processing, TSP 2012 - Proceedings* **2012**, pp. 513–516.

52. Bandt, C.; Pompe, B. Permutation Entropy: A Natural Complexity Measure for Time Series. *Physical Review Letters* **2002**, *88*, 174102.

53. Nicolaou, N.; Georgiou, J. Permutation entropy: A new feature for brain-computer interfaces. 2010 IEEE Biomedical Circuits and Systems Conference, BioCAS 2010. IEEE, 2010, pp. 49–52.

54. Unakafova, V.; Keller, K. Efficiently Measuring Complexity on the Basis of Real-World Data. *Entropy* **2013**, *15*, 4392–4415.

55. Berger, S.; Schneider, G.; Kochs, E.F.; Jordan, D. Permutation entropy: Too complex a measure for EEG time series? *Entropy* **2017**, *19*, 692.

56. Lowe, G. SIFT - The Scale Invariant Feature Transform. *International Journal* **2004**, *2*, 91–110.

57. Edelman, S.; Intrator, N.; Poggio, T. Complex cells and Object Recognition.

58. Ramele, R.; Villar, A.J.; Santos, J.M. BCI classification based on signal plots and SIFT descriptors. 4th International Winter Conference on Brain-Computer Interface, BCI 2016; IEEE: Yongpyong, 2016; pp. 1–4.

59. Zhang, R.; Xu, P.; Guo, L.; Zhang, Y.; Li, P.; Yao, D. Z-Score Linear Discriminant Analysis for EEG Based Brain-Computer Interfaces. *PLoS ONE* **2013**, *8*, e74433.

60. Vedaldi, A.; Fulkerson, B. VLFeat - An open and portable library of computer vision algorithms. *Design* **2010**, *3*, 1–4.

61. Quian Quiroga, R.; Garcia, H. Single-trial event-related potentials with wavelet denoising. *Clinical Neurophysiology* **2003**, *114*, 376–390.

62. Riccio, A.; Simione, L.; Schettini, F.; Pizzimenti, A.; Inghilleri, M.; Belardinelli, M.O.; Mattia, D.; Cincotti, F. Attention and P300-based BCI performance in people with amyotrophic lateral sclerosis. *Frontiers in Human Neuroscience* **2013**, *7*, 732.

63. Brunner, C.; Blankertz, B.; Cincotti, F.; Kübler, A.; Mattia, D.; Miralles, F.; Nijholt, A.; Otal, B. BNCI Horizon 2020 – Towards a Roadmap for Brain / Neural Computer Interaction. *Lecture Notes in Computer Science* **2014**, *8513*, 475–486.

64. Renard, Y.; Lotte, F.; Gibert, G.; Congedo, M.; Maby, E.; Delannoy, V.; Bertrand, O.; Lécuyer, A. OpenViBE: An Open-Source Software Platform to Design, Test, and Use Brain Computer Interfaces in Real and Virtual Environments. *Presence: Teleoperators and Virtual Environments* **2010**, *19*, 35–53.

65. Boiman, O.; Shechtman, E.; Irani, M. In defense of nearest-neighbor based image classification. *26th IEEE Conference on Computer Vision and Pattern Recognition, CVPR* **2008**.

66. Krusienski, D.J.; Sellers, E.W.; Cabestaing, F.; Bayoudh, S.; McFarland, D.J.; Vaughan, T.M.; Wolpaw, J.R. A comparison of classification techniques for the P300 Speller. *Journal of Neural Engineering* **2006**, *3*, 299–305.

67. Chavarriaga, R.; Fried-Oken, M.; Kleih, S.; Lotte, F.; Scherer, R. Heading for new shores! Overcoming pitfalls in BCI design. *Brain-Computer Interfaces* **2017**, *4*, 60–73.

68. Criminisi, A.; Shotton, J. *Decision forests for computer vision and medical image analysis*; Springer Science & Business Media, 2013.

69. Gu, S.; Jin, Y. Heterogeneous classifier ensembles for EEG-based motor imaginary detection. 2012 12th UK Workshop on Computational Intelligence, UKCI 2012. IEEE, 2012, pp. 1–8.

70. Skoog, D.A.; West, D.M.; Holler, F.J.; Crouch, S.R. Analytical chemistry: an introduction. *Saunders College Publishing: Philadelphia* **2000**.

71. Owens, T.J.; Zandt, G.; Taylor, S.R. Seismic evidence for an ancient rift beneath the Cumberland Plateau, Tennessee: A detailed analysis of broadband teleseismic P waveforms. *Journal of Geophysical Research: Solid Earth* **1984**, *89*, 7783–7795.

72. Stockman, G.; Kanal, L.; Kyle, M. Structural pattern recognition of carotid pulse waves using a general waveform parsing system. *Communications of the ACM* **1976**, *19*, 688–695.